Check for updates

OPEN

Dual frequency sound absorption with an array of shunt loudspeakers

Pengju Zhang[1,4], Chaonan Cong[2,4], Jiancheng Tao[1✉] & Xiaojun Qiu[3]

Transformer noise is dominated by low frequency components, which are hard to be controlled with traditional noise control approaches. The shunt loudspeaker consisting of a closed-box loudspeaker and a shunt circuit has been proposed as an effective sound absorber by storing and dissipating the electrical energy converted from the incident sound. In this paper, an array of shunt loudspeakers is proposed to control the 100 Hz and 200 Hz components of transformer noise. The prototype under tests has a thickness of 11.8 cm, which is only 1/28 of the wavelength of 100 Hz. The sound absorption performance of the array under random incidence is analyzed with the parallel impedance method, and the arrangement of array elements is optimized. The test results in a reverberation room show that the proposed array has sound absorption coefficients of 1.04 and 0.93 at 100 Hz and 200 Hz, respectively, which provides potential of applying this type of thin absorbers for low-frequency sound control.

Effective absorption of the low frequency sound is a challenge in noise control and architectural acoustics. Traditional absorbers usually require large back cavity or thick depth for low frequency sound absorption[1–5]. Acoustic metamaterials have been studied intensively due to their subwavelength size[6–20]. For example, thickness of metamaterial absorbers can be significantly reduced with space coiling or folding[6–9]; however, the absorption performance is hard to be tuned after they are manufactured[8,10]. Membrane based metamaterials[11–13] and resonance coupling metamaterials[14–18] require specific elastic properties or Q-factors to attain optimal absorption performance, but they are difficult to be manufactured for large-scale applications. Active noise control technology[21–23] has problems of the system cost, complexity and robustness.

A typical shunt loudspeaker (SL) is composed of a closed-box loudspeaker with a shunt circuit connected to its terminals. Its absorption performance can be adjusted by tuning the shunt circuit. The SL was firstly proposed for the sound field control in a duct[24] and its working mechanism was proven to be equal to that of a feedback active control system[25]. Negative impedance converters were employed to adjust the SLs flexibly by tuning the negative resistances, inductances or capacitances implemented in the shunt circuit[26], and micro-perforated panels were combined to extend the absorption frequency band of the SLs[27,28]. Dual-resonance and multi-resonance absorbing SLs were also investigated for multi-tonal noise absorption[29–31], where the normal absorption coefficients of the designed SL are larger than 0.9 at 100 Hz and its harmonic frequencies. These results demonstrate that a single SL can be an effective and adjustable sound absorber. For practical applications, multiple SLs have to be used. Although several SLs have been used for the room mode equalizations[32,33], the sound absorption performance of SL arrays under the random incidence is unknown, which is reported in this paper.

Results

Figure 1a shows an element of the SL array, which has a thickness of 11.8 cm and targets at 100 Hz and 200 Hz sound absorption. In the figure, $-R_E$, C_1 and L_1 are negative shunt resistance, shunt capacitance and shunt inductance, respectively. The side length of the square front surface of the SL is 16.3 cm and the effective radius of the loudspeaker diaphragm is 5 cm. The Thiele-Small (TS) parameters[34,35] of the loudspeaker driver and the electrical parameters of the shunt circuit are provided in the Supplementary Information. The normal absorption coefficient of each element in the array is calculated analytically (the details are listed in "The analytical method" section), simulated numerically (the details are listed in "The simulation method" section), and measured experimentally (the details are listed in "The measurement method" section), and the results are shown in Fig. 1b. The averaged

[1]Key Laboratory of Modern Acoustics and Institute of Acoustics, Nanjing University, Nanjing, China. [2]Department of Physics, China Jiliang University, Hangzhou, China. [3]Centre for Audio, Acoustics and Vibration, Faculty of Engineering and IT, University of Technology Sydney, Sydney, Australia. [4]These authors contributed equally: Pengju Zhang and Choanan Cong. ✉email: jctao@nju.edu.cn
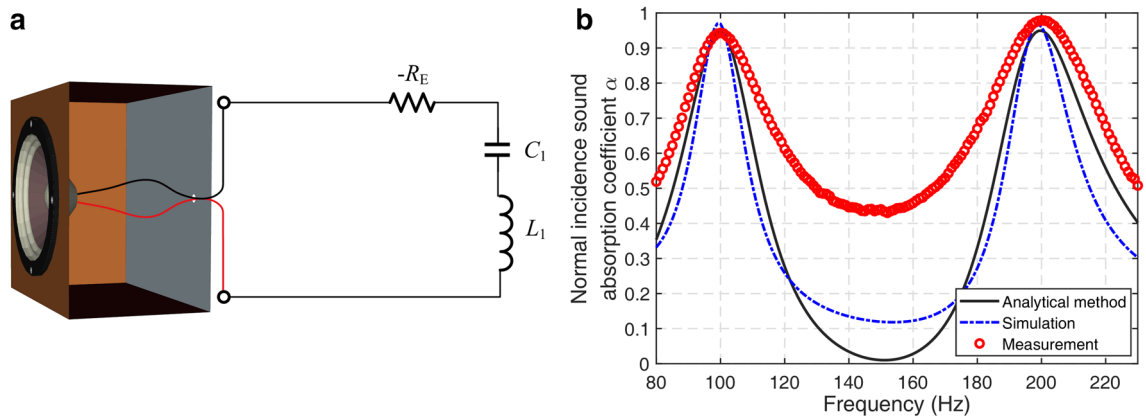
1

Figure 1. (**a**) The schematic of an element of the SL array for dual frequency sound absorption, (**b**) typical normal absorption coefficients of an element of the designed SL array [drawn with Microsoft Visio 2019 (https ://itsc.nju.edu.cn/Visio/list.htm), MATLAB 2019a (https://itsc.nju.edu.cn/21628/list.htm) and Adobe Illustrator CC 2018 (https://itsc.nju.edu.cn/adobe/list.htm)].
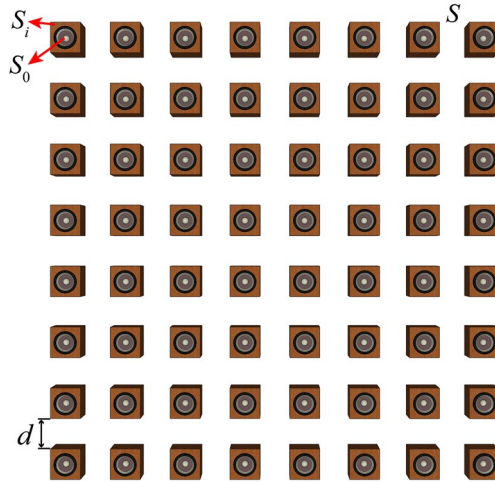
Figure 2. The schematic diagram of the SL array [drawn with Adobe Illustrator CC 2018 (https://itsc.nju.edu.cn/adobe/list.htm)].

values of the measured normal absorption coefficients agree well with that from the theory and simulations, and the values at 100 Hz and 200 Hz are 0.94 and 0.97, respectively.

Figure 2 shows the SL array made with 64 elements distributed evenly in an area of S, where S_0 is the effective area of the speaker diaphragm, S_i is the area of the front surface of the ith element, and d is the interval between the elements. Define the area ratio σ as the ratio between the total effective area of the loudspeaker's diaphragms to the area of the array S. The area ratio σ reaches the maximum value of 1 if $d = 0$ and S_i equals to S_0, but for practical closed-box loudspeakers with a circular diaphragm, σ is less than $\pi/4$.

Five layout patterns with different intervals of 33 cm, 25 cm, 16.5 cm, 8.3 cm and 0 cm were investigated and the random incident absorption coefficient was measured in the reverberation room. The optimal layout with the largest absorption coefficients at 100 Hz and 200 Hz is illustrated in Fig. 3a. In this layout, the interval between SLs is $d = 0$ m and the total area of the array is $S = 1.74$ m². The random incident absorption coefficient of the array is 1.04 at 100 Hz and 0.93 at 200 Hz as shown in Fig. 3d. The main reason for the measured absorption coefficient in Fig. 3d to be greater than 1 is the extra sound absorption caused by the diffraction from the edges of the test sample to the incident sound wave[36].

Figure 3b, c show two of the other four layout patterns with intervals of 16.5 cm and 33 cm, respectively. The areas of these two arrays are 6.10 m² and 13.25 m², so the area ratio σ are 0.082 and 0.038, respectively. The random incident absorption coefficients of the SL arrays with these two layouts are shown in Fig. 3e, f. The test results demonstrate that the proposed SL array has a good absorption performance while its thickness is only approximately 1/28 wavelength of 100 Hz.
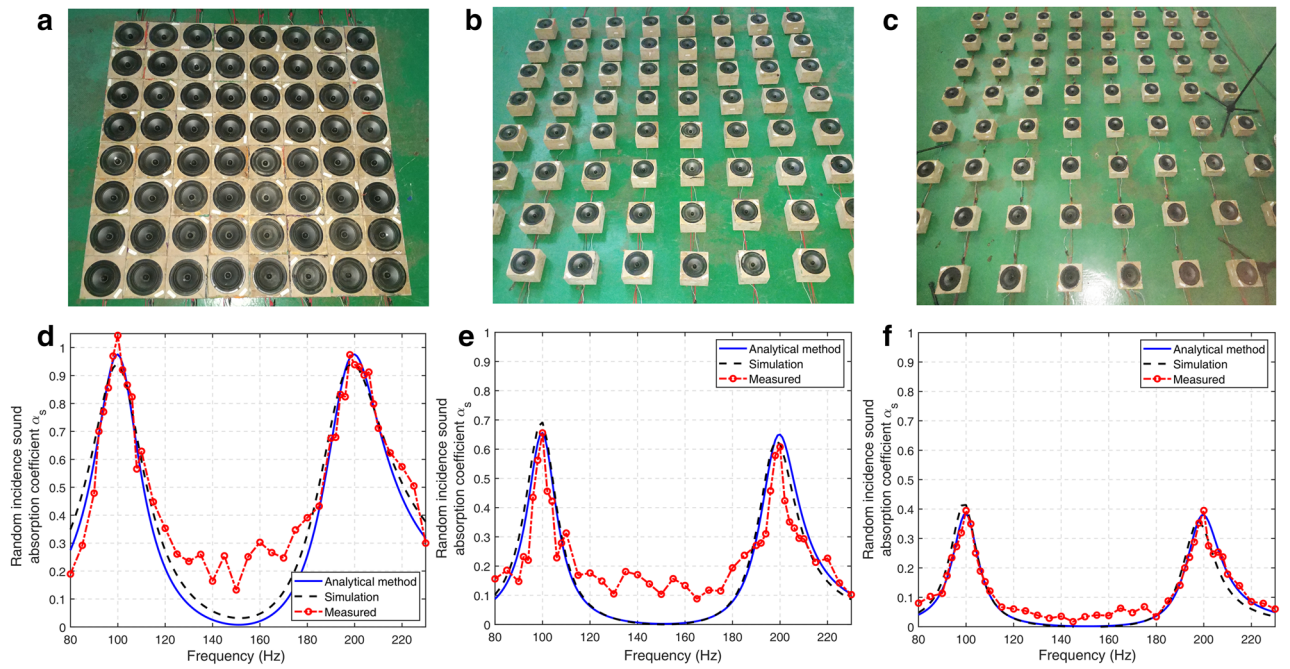
Figure 3. (**a**) The optimal layout of the SL array, (**b**) the SL array with the interval of 16.5 cm, (**c**) the SL array with the interval of 33 cm, (**d**) random incident absorption coefficient corresponding to configuration in (**a**), (**e**) random incident absorption coefficient corresponding to configuration in (**b**), (**f**) random incident absorption coefficient corresponding to configuration in (**c**) [drawn with MATLAB 2019a (https://itsc.nju.edu.cn/21628/list.htm) and Adobe Illustrator CC 2018 (https://itsc.nju.edu.cn/adobe/list.htm)].
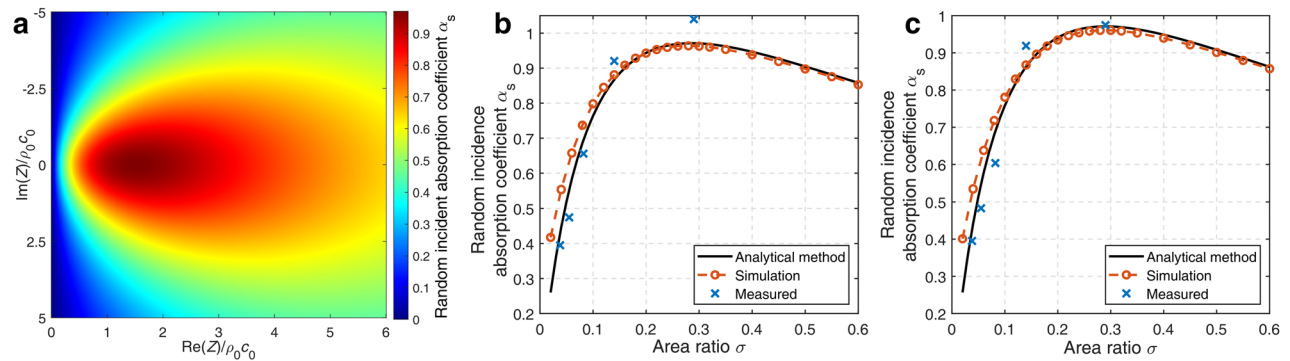

Figure 4. (**a**) The random incident absorption coefficient for the array of SLs with different acoustic impedance ratios, (**b**)–(**c**) random incident absorption efficient of the SL array with different area ratios at target frequencies (**b**) at 100 Hz (**c**) at 200 Hz [drawn with MATLAB 2019a (https://itsc.nju.edu.cn/21628/list.htm) and Adobe Illustrator CC 2018 (https://itsc.nju.edu.cn/adobe/list.htm)].

Discussions

The absorption coefficients of the SL array are determined by the properties of elements and their layout. The equivalent acoustic impedance Z of the array can be derived as

$$Z \approx \frac{Z_{SL}}{\sigma} \tag{1}$$

using the analytical method described in the "Methods" section, where Z_{SL} is the equivalent acoustic impedance of the SL. Figure 4a shows the random incident absorption coefficient of the SL array as a function of the equivalent acoustic impedance. When the real part of Z equals $1.51\rho_0 c_0$ and the imaginary part of Z is zero, where $\rho_0 c_0$ is the characteristic acoustics impedance of air, the random incident absorption coefficient reaches a maximum value close to 0.97. As shown in Eq. (1), the equivalent acoustic impedance of the array is affected by the area ratio, so the maximum random incident absorption coefficient can be achieved by adjusting the area ratio σ when the real part of Z_{SL} is smaller than $1.51\rho_0 c_0$. The optimal area ratio σ_{opt} is
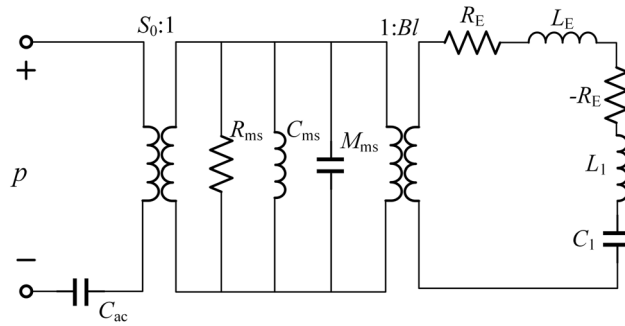
Figure 5. The equivalent circuit model of the designed SL prototype [drawn with Microsoft Visio 2019 (https://itsc.nju.edu.cn/Visio/list.htm)].

$$\sigma_{\text{opt}} = \frac{\text{Re}(Z_{\text{SL}})}{1.51\rho_0 c_0} = 0.66\frac{\text{Re}(Z_{\text{SL}})}{\rho_0 c_0}, \tag{2}$$

where $\text{Re}(Z_{\text{SL}})$ denotes the real part of Z_{SL}.

Figure 4b,c shows the random incident absorption coefficients of the array with different area ratios at 100 Hz and 200 Hz, respectively, where the markers with "×" represent the measurement results. The theory and simulation results show that the random incident absorption coefficient increases first and then decreases with the area ratio σ, and the maximum absorption coefficient is 0.97 when the area ratio is 0.29 for both 100 Hz and 200 Hz. In the experiments, the maximal absorption coefficient at 100 Hz and 200 Hz appears when the interval is 0 cm as shown in Fig. 3a and the corresponding area ratio is 0.29. The optimal area ratio agrees well with the calculated value of 0.29 from Eq. (2).

In conclusion, the sound absorption coefficients of an array of shunt loudspeakers under random incidence were tested in a reverberation room and the results were analyzed with the parallel impedance method. With the optimized arrangement of the array elements, the proposed array achieves sound absorption coefficients of 1.04 and 0.93 at 100 Hz and 200 Hz, respectively, but with a thickness of only 1/28 of the wavelength of 100 Hz. It is demonstrated that an array of shunt loudspeakers can be designed as thin sound absorbers for low frequency noise control.

Methods

The analytical method.   The equivalent acoustic impedance of the SL can be derived by using the equivalent circuit model[27]. Figure 5 shows the equivalent circuit model of a SL, where p is the incident pressure acting on the diagram, Bl is electromechanical coupling factor, R_{E} is the DC electrical resistance of the voice coil, L_{E} is the equivalent inductance of the voice coil, R_{ms} is the force resistance of the loudspeaker suspension system, M_{ms} is the mass of the driver cone, C_{ms} is the force compliance of the suspension system, and S_0 is the effective area of the driver cone. C_{ac} is the equivalent acoustic capacitance of the back cavity with volume V and $C_{\text{ac}} = V/\rho_0 c_0^2$. The values of all these parameters are given in the Supplementary Information. The acoustic impendence Z_{SL} at the diaphragm can be described by

$$Z_{\text{SL}} = \frac{R_{\text{ms}}}{S_0} + \frac{j\omega M_{\text{ms}}}{S_0} + \left(\frac{1}{j\omega C_{\text{ms}}S_0^2} + \frac{1}{j\omega C_{ac}}\right)S_0 + \frac{(Bl)^2}{S_0\left[j\omega(L_{\text{E}}+L_1) + 1/j\omega C_1\right]}, \tag{3}$$

Assume Z_{W} is the acoustic impedance of the wooden plate with a thickness of 0.9 cm to make up the closed box, the equivalent acoustic impedance of each SL element can be obtained by

$$Z_i = \frac{S_i}{\left(\frac{S_0}{Z_{\text{SL}}} + \frac{S_i - S_0}{Z_{\text{W}}}\right)}. \tag{4}$$

The acoustic impedance of each space between SLs in the array can be obtained by[37]

$$Z_s = \frac{\rho_0 c_0}{j \tan kh} \tag{5}$$

where k and h are the wave number and the thickness of the array respectively. The equivalent acoustic impedance of the whole SL array is

$$Z = \frac{S}{\sum_{i=1}^{64} \left(\frac{1}{Z_i/S_i}\right) + \frac{1}{Z_s/(S-64S_i)}} \tag{6}$$

When all SL elements are identical, using the relationship that $Z_{\text{W}} \gg Z_{\text{SL}}$ and $kh \ll 1$, Eq. (6) can be approximated as Eq. (1). And the random incident absorption coefficient α_{s} can be calculated by[38]
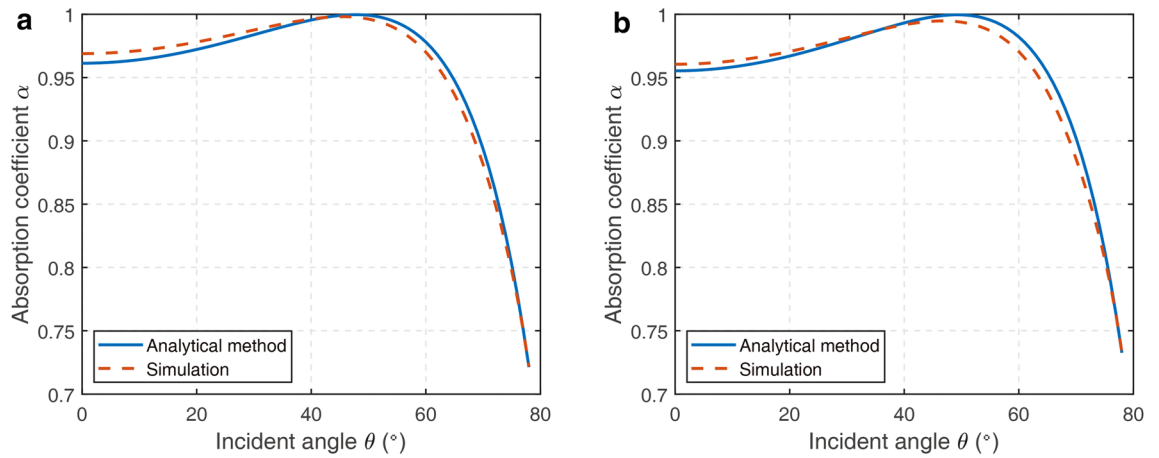
Figure 6. Oblique incident absorption coefficient with different incident angle when the space between the elements is $d = 0$ cm (**a**) at 100 Hz (**b**) at 200 Hz [drawn with MATLAB 2019a (https://itsc.nju.edu.cn/21628/list.htm)].
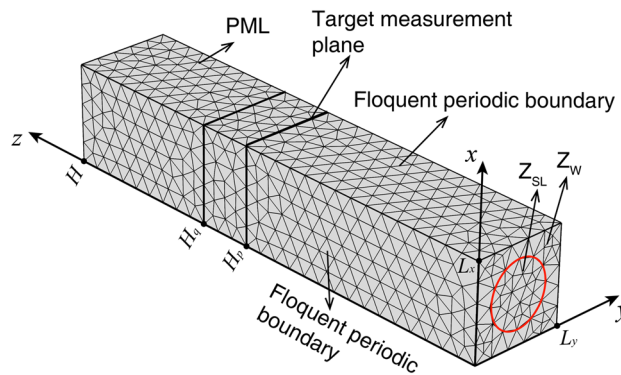

Figure 7. The finite element simulation model used in the research [drawn with COMSOL Multiphysics 5.4 (www.comsol.com) and Adobe Illustrator CC 2018 (https://itsc.nju.edu.cn/adobe/list.htm)].

$$\alpha_s = \frac{\int_0^{78°} \alpha(\theta) \sin(2\theta) d\theta}{\int_0^{78°} \sin(2\theta) d\theta} \tag{7}$$

where the absorption coefficient of the SL array for the oblique incidence with an angle θ can be obtained by[37]

$$\alpha(\theta) = \frac{4\rho_0 c_0 \mathrm{Re}(Z) \cos\theta}{[\rho_0 c_0 + \mathrm{Re}(Z) \cos\theta]^2 + [\mathrm{Im}(Z) \cos\theta]^2} \tag{8}$$

Figure 6 shows the calculated oblique incident absorption coefficient of the SL array at different incident angles at 100 Hz and 200 Hz when the space between the elements is $d = 0$ m. The simulation results are obtained with COMSOL Multiphysics. The absorption coefficients increase first and then decrease with the incident angle. The maximal oblique absorption coefficient at 100 Hz occurs at $\theta = 48°$ (Analytical method)/47° (Simulation), while the maximum at 200 Hz occurs at $\theta = 49°$ (Analytical method)/47° (Simulation).

The simulation method. In order to validate the analytical model, a numerical approach is adopted based on the Finite Element Method (FEM). The finite element simulation model established in COMSOL Multiphysics 5.3a is shown in Fig. 7. The surface at $z = 0$ is set as the impedance boundary, where the acoustic impedance in the middle circular region with radius of 5 cm is set as Z_{SL} and the rest area is set as a rigid wall. The region with $0 < z < H_q$ is set as the plane wave radiating sound field and the target measurement plane is $z = H_p$. The region with $H_q < z < H$ is set as a Perfectly Matched Layer (PML), which prevent the sound wave from reflecting when it propagates to the plane of $z = H_q$. Thus, we can simulate a free field condition. The side surfaces with $x = 0, L_x$ and $y = 0, L_y$ are set as Floquent periodic boundaries, which makes the simulation model repeat periodically in both x and y directions. Thus, we can simulate an array with infinitely many shunt loudspeakers. The parameters H, H_q, and H_p are set as 0.9 m, 0.6 m and 0.5 m respectively and L_x, L_y are determined by different area ratio σ. The maximum element size is set as 3.43 cm and the geometric model is divided into 10,749 domain elements, 1,692 boundary elements, and 315 edge elements for numerical calculation.
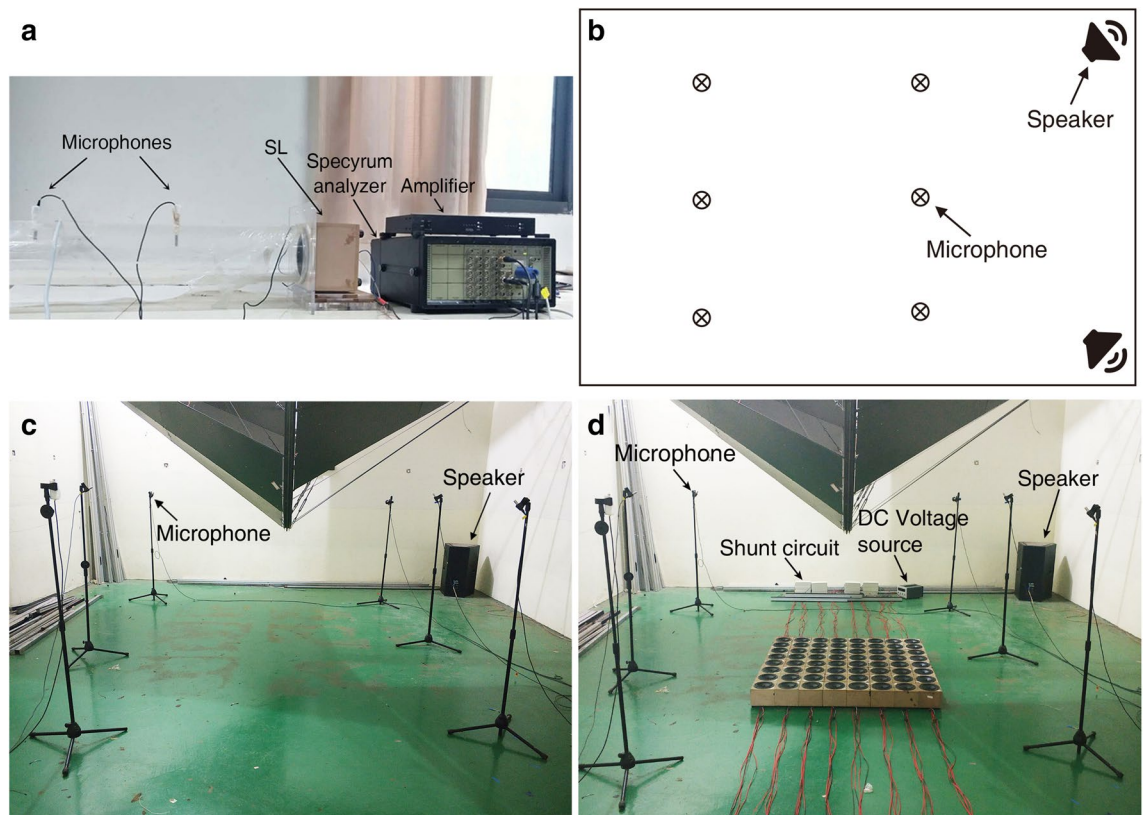
5

Figure 8. (**a**) Measurement apparatus for normal absorption coefficients, (**b**) the position of the microphones and the sound sources in the reverberation room, (**c**, **d**) the photo of the measurement setup without (**c**) and with (**d**) the shunt loudspeaker array in the reverberation room [drawn with Adobe Illustrator CC 2018 (https://itsc.nju.edu.cn/adobe/list.htm)].

When a background plane wave sound field with an incident angle θ is applied at the region of $0 < z < H_q$, the incident sound pressure p_{inc} and the reflected sound pressure p_{scat} on the target measurement plane at $z = H_p$ are calculated. The sound absorption coefficient $\alpha(\theta)$ could be obtained as

$$\alpha(\theta) = 1 - \left(\frac{p_{inc}}{p_{scat}}\right)^2. \tag{9}$$

The normal absorption coefficient can be calculated by Eq. (9) when the incident angle θ is 0°, and the random incident absorption coefficient is calculated by Eqs. (9) and (7) when the incident angle θ is swept between 0° and 78° with a step of 1°.

The measurement method. The normal incident absorption coefficient was measured in an impedance tube according to ISO 10534-2[39] with a B&K PULSE 3560D analyzer as shown in Fig. 8a. The sound source is fixed at the other end of the pipe and cannot be seen in the figure. The pipe is made of acrylic with a thickness of 15 mm, which can be considered as a rigid wall, because the acoustic characteristic impedance of acrylic is much larger than that of air. The diameter of the pipeline is 12 cm and the distance of the two microphones is 30 cm.

The measurement of the random incident absorption coefficient was conducted in the reverberation room of the Institute of Acoustics of Nanjing University and the sound source interruption method according to ISO 354:2003[40] was adopted with a B&K PULSE 3560D analyzer. The volume of the reverberation chamber is 224.8 m³. The temperature and the relative humidity of air during the measurements were 25 °C and 72% respectively. Two β_3-MU15 speakers manufactured by Elder Audio Manufacture Co., Ltd were used as the sound sources and placed at the corners of the reverberation room. Six microphones produced by Beijing AcousticSensing Technology Ltd were evenly placed in the reverberation room with a height of 1.2 m. The positions of the microphones and the sound sources are illustrated in Fig. 8b. The tonal sound ranging from 80 and 230 Hz with a step of 5 Hz was used in the measurements and the frequency step is reduced to 2 Hz between 90 and 110 Hz and between 190 and 210 Hz for better frequency resolution. Each measurement is repeated three times for averaging. A panoramic view of the measurement system without and with the SL array is shown in Fig. 8c,d, respectively.

Data availability
All data generated or analyzed during this study are included in this published article (and its Supplementary Information files).

References

1. Moore, J. A. & Lyon, R. H. Resonant porous material absorbers. *J. Acoust. Soc. Am.* **72**, 1989–1999 (1982).
2. Maa, D. Y. Potential of microperforated panel absorber. *J. Acoust. Soc. Am.* **104**, 2861–2866 (1998).
3. Lee, D. H. & Kwon, Y. P. Estimation of the absorption performance of multiple layer perforated panel systems by transfer matrix method. *J. Sound Vib.* **278**, 847–860 (2004).
4. Zhao, X. & Fan, X. Enhancing low frequency sound absorption of micro-perforated panel absorbers by using mechanical impedance plates. *Appl. Acoust.* **88**, 123–128 (2015).
5. Fenech, B., Keith, G. M. & Jacobsen, F. The use of microperforated plates to attenuate cavity resonances. *J. Acoust. Soc. Am.* **120**, 1851–1859 (2006).
6. Donda, K. *et al.* Extreme low-frequency ultrathin acoustic absorbing metasurface. *Appl. Phys. Lett.* **115**, 173506 (2019).
7. Cai, X., Guo, Q., Hu, G. & Yang, J. Ultrathin low-frequency sound absorbing panels based on coplanar spiral tubes or coplanar Helmholtz resonators. *Appl. Phys. Lett.* **105**, 121901 (2014).
8. Wu, X. *et al.* Low-frequency tunable acoustic absorber based on split tube resonators. *Appl. Phys. Lett.* **109**, 043501 (2016).
9. Zhou, Y., Li, D., Li, Y. & Hao, T. Perfect acoustic absorption by subwavelength metaporous composite. *Appl. Phys. Lett.* **115**, 093503 (2019).
10. Yang, M., Chen, S., Fu, C. & Sheng, P. Optimal sound-absorbing structures. *Mater. Horiz.* **141**, 3575–3575 (2016).
11. Yang, Z., Dai, H. M., Chan, N. H., Ma, G. C. & Sheng, P. Acoustic metamaterial panels for sound attenuation in the 50–1000 Hz regime. *Appl. Phys. Lett.* **96**, 041906 (2010).
12. Duan, Y. *et al.* Theoretical requirements for broad tic waves by ultra-thin elastic meta-films. *Sci. Rep.* **5**, 12139 (2015).
13. Mei, J. *et al.* Dark acoustic metamaterials as super absorbers for low-frequency sound. *Nat. Commun.* **3**, 756 (2012).
14. Yang, M. *et al.* Subwavelength total acoustic absorption with degenerate resonators. *Appl. Phys. Lett.* **107**, 104104 (2015).
15. Ma, G., Yang, M., Xiao, S., Yang, Z. & Sheng, P. Acoustic metasurface with hybrid resonances. *Nat. Mater.* **13**, 873–878 (2014).
16. Wei, P., Croenne, C., Chu, S. T. & Li, J. Symmetrical and anti-symmetrical coherent perfect absorption for acoustic waves. *Appl. Phys. Lett.* **104**, 121902 (2014).
17. Jiang, X. *et al.* Ultra-broadband absorption by acoustic metamaterials. *Appl. Phys. Lett.* **105**, 243505 (2014).
18. Jiménez, N., Romero-García, V., Pagneux, V. & Groby, J. P. Rainbow-trapping absorbers: broadband, perfect and asymmetric sound absorption by subwavelength panels for transmission problems. *Sci. Rep.* **7**, 13595 (2017).
19. Gu, Z. *et al.* Experimental realization of broadband acoustic omnidirectional absorber by homogeneous anisotropic metamaterials. *J. Appl. Phys.* **117**, 074502 (2015).
20. Li, R. Q. *et al.* A broadband acoustic omnidirectional absorber comprising positive-index materials. *Appl. Phys. Lett.* **99**, 193507 (2011).
21. Nelson, P. & Elliott, S. *Active Control of Sound* (Academic Press, Massachusetts, 1993).
22. Elliott, S. *Signal Processing for Active Control* (Academic Press, New York, 2001).
23. Zhu, H., Rajamani, R. & Stelson, K. A. Active control of acoustic reflection, absorption, and transmission using thin panel speakers. *J. Acoust. Soc. Am.* **113**, 852–870 (2003).
24. Fleming, A. J., Niederberger, D., Moheimani, S. R. & Morari, M. Control of resonant acoustic sound fields by electrical shunting of a loudspeaker. *IEEE Trans. Control Syst. Technol.* **15**(4), 689–703 (2007).
25. Lissek, H., Boulandet, R. & Fleury, R. Electroacoustic absorbers: bridging the gap between shunt loudspeakers and active sound absorption. *J. Acoust. Soc. Am.* **129**, 2968–2978 (2011).
26. Černík, M. & Mokrý, P. Sound reflection in an acoustic impedance tube terminated with a loudspeaker shunted by a negative impedance converter. *Smart Mater. Struct.* **21**(11), 115016 (2012).
27. Tao, J., Jing, R. & Qiu, X. Sound absorption of a finite micro-perforated panel backed by a shunted loudspeaker. *J. Acoust. Soc. Am.* **135**, 231–238 (2014).
28. Zhang, Y., Chan, Y. J. & Huang, L. Thin broadband noise absorption through acoustic reactance control by electro-mechanical coupling without sensor. *J. Acoust. Soc. Am.* **135**, 2738–2745 (2014).
29. Jing, R., Tao, J. & Qiu, X. Shunted loudspeakers for transformer noise absorption. In *Proceedings of the 21st International Congress on Sound and Vibration*, Vol. 2, 1160–1165 (2014).
30. Cong, C., Tao, J. & Qiu, X. Thin multi-tone sound absorbers based on analog circuit shunt loudspeakers. *Noise Control. Eng. J.* **66**, 496–504 (2018).
31. Cong, C., Tao, J. & Qiu, X. A Multi-Tone Sound Absorber Based on an Array of Shunted Loudspeakers. *Appl. Sci.* **8**, 2484 (2018).
32. Karkar, S. *et al.* Electroacoustic absorbers for the low-frequency modal equalization of a room: what is the optimal target impedance for maximum modal damping, depending on the total area of absorbers? In *Forum Acusticum* (2014).
33. Lissek, H., Boulandet, R., Rivet, E. & Rigas, I. Assessment of active electroacoustic absorbers as low frequency modal dampers in rooms. In *Proceedings of Inter-noise* (2012)
34. Thiele, N. Loudspeakers in vented boxes: Part 2. *J. Audio. Eng. Soc.* **19**(5), 471–483 (1971).
35. Small, R. H. Direct radiator loudspeaker system analysis. *J. Audio. Eng. Soc.* **20**(5), 383–395 (1972).
36. Dekker, H. Edge effect measurements in a reverberation room. *J. Sound. Vib.* **32**(2), 199–202 (1974).
37. Morse, P. M. & Ingard, K. U. *Theoretical Acoustics* (Academic Press, New York, 1968).
38. Sakagami, K., Yamashita, I., Yairi, M. & Morimoto, M. Effect of a honeycomb on the absorption characteristics of double-leaf microperforated panel (MPP) space sound absorbers. *Noise Control. Eng. J.* **59**(4), 363 (2011).
39. ISO 10534-2. Acoustics-Determination of Sound Absorption Coefficient and Impedance in Impedance Tubes. Part 2: Transfer Function Method (1998).
40. ISO 354. Acoustics-measurement of sound absorption in a reverberation room (2003).

Acknowledgements

Author contributions

P.Z. and C.C. completed the main work of this manuscript under J.T. and X.Q.'s guidance. X.Q. and J.T. initiated the research, P.Z. and C.C. derived the formulations and carried out the experiments, P.Z. wrote the paper draft under J.T. and X.Q.'s guidance and finalized the paper. All authors reviewed the manuscript.

Competing interests

The authors declare no competing interests.

Additional information

Supplementary information is available for this paper at https://doi.org/10.1038/s41598-020-67810-z.

Correspondence and requests for materials should be addressed to J.T.

Reprints and permissions information is available at www.nature.com/reprints.

Publisher's note Springer Nature remains neutral with regard to jurisdictional claims in published maps and institutional affiliations.